



Preparation, structure and electrochemical behavior of dinuclear cyclooctadiene-chelated Ir(I) complexes with 2-aminopyridinato bridges

Naohiro Kanematsu, Masahiro Ebihara, Takashi Kawamura *

Department of Chemistry, Faculty of Engineering, Gifu University, Yanagido, Gifu 501-1193, Japan

Received 14 January 1999; accepted 23 April 1999

Abstract

Dinuclear iridium(I) complexes with two bridging aminopyridinato ligands, $[\text{Ir}(\mu\text{-L})(\text{COD})]_2$ (COD = 1,5-cyclooctadiene (**1**): L = 2-aminopyridinato (ap) (**2**): L = 2-anilinopyridinato (anp)), were prepared from $[\text{Ir}(\mu\text{-Cl})(\text{COD})]_2$ and Li^+L^- in a 24–36% yield. These compounds were characterized by X-ray structure analysis and ^1H NMR spectroscopy. Two iridium atoms were bridged by two aminopyridinato ligands and each iridium atom was coordinated by one chelating COD. The coordination sphere of each Ir(I) center, which was formed by two N atoms and two olefinic π bonds, was square planar. Ir...Ir separations in **1** and **2** were 3.0998(6) and 3.0681(3) Å, respectively. Cyclic voltammetry of **1** and **2** in $n\text{-Bu}_4\text{NPF}_6/\text{CH}_2\text{Cl}_2$ exhibited a chemically reversible oxidation wave at -0.41 and -0.36 V versus Fc^+/Fc , respectively. These potentials were lower than those of $[\text{Ir}(\mu\text{-form})(\text{COD})]_2$ (form = anion of *N,N'*-di-*p*-tolylformamidine), $[\text{Ir}(\mu\text{-hp})(\text{COD})]_2$ (hp = anion of 2-hydroxypyridine), $[\text{Ir}(\mu\text{-mhp})(\text{COD})]_2$ (mhp = anion of 6-methyl-2-hydroxypyridine) and $[\text{Ir}(\mu\text{-pz})(\text{COD})]_2$ (pz = anion of pyrazole). Electrolytic one-electron oxidation of **2** gave its stable cationic radical, $[\text{Ir}(\mu\text{-anp})(\text{COD})]_2^+$, of which frozen solution ESR spectrum was rhombic with $g_1 = 2.43$, $g_2 = 2.30$ and $g_3 = 2.08$ and no hyperfine splitting was resolved. © 1999 Elsevier Science S.A. All rights reserved.

Keywords: Crystal structures; Electrochemistry; Iridium complexes; Aminopyridinato complexes; Dinuclear complexes

1. Introduction

A variety of lantern type dinuclear complexes have been synthesized and characterized in the last three decades [1]. Although the chemistry of lantern type Rh(II) dinuclear complexes with a variety of ligands has been extensively studied [1], only a few of the corresponding dinuclear complexes of Ir(II) have been reported [2]. Since metal–metal and metal–ligand electronic interactions are expected to be enhanced in 5d metal complexes, we considered that development of synthetic route of Ir(II) dimers is an important field. We are interested in Ir(I) dimers, $[\text{Ir}(\mu\text{-L})(\text{COD})]_2$, as a starting material for Ir(II) complexes. $[\text{Ir}(\mu\text{-L})(\text{COD})]_2$ complexes have been synthesized by the substitution reaction of $[\text{Ir}(\mu\text{-Cl})(\text{COD})]_2$ with ligands such as form [3], hp [4], mhp [4,5], pz [6,7], mpz (anion of 2-mercap-

tothiazoline) [8] and mpm (anion of (6-methyl-2-pyridyl)methyl) [9] and yields were 55–90%. In terms of oxidation of Ir(I) complexes to Ir(II) species, complexes with strong donor ligands such as aminopyridinato ligands are expected to facilitate their oxidation. We report here on the synthesis, structure and electrochemistry of Ir(I) dinuclear complexes with 2-aminopyridinato and 2-anilinopyridinato ligands.

2. Experimental

2.1. General

All operations were carried out under an argon atmosphere using the standard Schlenk line techniques. Solvents were distilled from P_2O_5 . 2-Aminopyridine and 2-anilinopyridine were recrystallized from hexane. $[\text{Ir}(\mu\text{-Cl})(\text{COD})]_2$ was prepared by following a literature method [10].

* Corresponding author. Tel.: +81-58-239 2567; fax: +81-58-230 1893.

Table 1
Crystallographic data for $[\text{Ir}(\mu\text{-ap})(\text{COD})]_2$ (**1**) and $[\text{Ir}(\mu\text{-anp})(\text{COD})]_2$ (**2**)

	1	2
Empirical formula	$\text{C}_{26}\text{H}_{34}\text{Ir}_2\text{N}_4$	$\text{C}_{38}\text{H}_{42}\text{Ir}_2\text{N}_4$
Formula weight	787.02	939.22
Crystal color	dark red	dark red
Crystal dimensions (mm ³)	0.30 × 0.10 × 0.05	0.65 × 0.10 × 0.10
Space group	$P\bar{1}$ (no. 2)	$P\bar{1}$ (no. 2)
<i>a</i> (Å)	9.975(2)	10.506(1)
<i>b</i> (Å)	14.573(3)	18.138(2)
<i>c</i> (Å)	9.108(1)	9.1563(8)
α (°)	97.14(2)	96.882(8)
β (°)	110.71(1)	114.034(6)
γ (°)	101.57(2)	86.263(9)
<i>V</i> (Å ³)	1185.5(4)	1581.8(3)
<i>Z</i>	2	2
ρ_{calc} (g cm ⁻³)	2.205	1.972
μ (Mo K α) (cm ⁻¹)	112.67	84.62
Temperature (°C)	-80	-80
No. unique data	5427	7253
Data with $I > 2\sigma(I)$	3848	6028
No. of variables	290	398
Transmission factors, min./max.	0.332/0.569	0.195/0.429
<i>R</i> ^a	0.039	0.033
<i>R</i> _w ^b	0.046	0.044
Goodness-of-fit indicator ^c	1.19	1.56

$$^a R = \sum \|F_o\| - |F_c| / \sum \|F_o\|$$

$$^b R_w = [\sum w(|F_o| - |F_c|)^2 / \sum w|F_o|^2]^{1/2}; w = 1/\sigma^2(|F_o|)$$

$$^c \text{Goodness-of-fit indicator} = [\sum w(|F_o| - |F_c|)^2 / (N_{\text{obs}} - N_{\text{parameters}})]^{1/2}$$

2.2. Preparation of $[\text{Ir}(\mu\text{-ap})(\text{COD})]_2$ (**1**)

A solution of lithium 2-aminopyridinate which was prepared by stirring 2-aminopyridine (0.059 g, 0.63 mmol) and t-BuLi (0.45 ml of 1.7 M solution in pentane, 0.68 mmol) in toluene (10 ml) for 1 h at room temperature (r.t.) was added to $[\text{Ir}(\mu\text{-Cl})(\text{COD})]_2$ (0.20 g, 0.29 mmol). After stirring for 12 h the resulting dark-red solution was filtered and evaporated to dryness. The dark-red residue was recrystallized from hexane to give **1** as dark-red crystals: yield 0.054 g (24%). *Anal.* Calc. for $\text{C}_{26}\text{H}_{34}\text{Ir}_2\text{N}_4$: C, 39.68; H, 4.35; N, 7.12. Found: C, 39.43; H, 4.48; N, 6.95%. ¹H NMR (CD_2Cl_2 , -40°C, ppm) δ 7.74 (d, 2H), 6.81 (t, 2H), 6.08 (d, 2H), 6.00 (t, 2H), 4.74 (br, 2H), 3.71 (br, 2H), 3.58 (br, 2H), 3.52 (br, 2H), 2.71 (br, 2H), 2.59 (br, 2H), 2.29 (br, 4H), 1.92 (br, 2H), 1.74 (br, 4H), 1.32 (br, 4H). At r.t. the COD resonances exhibited fluxional behavior.

2.3. Preparation of $[\text{Ir}(\mu\text{-anp})(\text{COD})]_2$ (**2**)

The preparation was similar to that of $[\text{Ir}(\mu\text{-ap})(\text{COD})]_2$. Starting materials of $[\text{Ir}(\mu\text{-Cl})(\text{COD})]_2$ (0.20 g, 0.30 mmol), Hanp (0.10 g, 0.59 mmol) and t-BuLi (0.35 ml of 1.7 M solution in pentane, 0.60 mmol) gave **2** as dark-red crystals: yield 0.10 g (36%). *Anal.* Calc. for

$\text{C}_{38}\text{H}_{42}\text{Ir}_2\text{N}_4$: C, 48.60; H, 4.51; N, 5.97. Found: C, 48.62; H, 4.55; N, 5.90%. ¹H NMR (CD_2Cl_2 , 20°C, ppm) δ 8.26 (d, 2H), 7.41 (br, 8H), 7.15 (m, 2H), 6.72 (t, 2H), 6.03 (t, 2H), 5.67 (d, 2H), 4.17 (m, 2H), 3.80 (m, 2H), 3.27 (m, 2H), 2.89 (m, 2H), 2.62 (br, 4H), 2.10 (m, 2H), 2.00 (m, 2H), 1.59 (m, 6H), 1.39 (m, 2H).

2.4. Crystallography

Crystallographic data and details of the structure refinement for **1** and **2** are summarized in Table 1. Intensity data were collected on a Rigaku AFC7R diffractometer by the ω - 2θ scan method in the range $4 < 2\theta < 55^\circ$ with Mo K α radiation ($\lambda = 0.71069$ Å). All calculations were performed by using a TEXSAN crystallographic software package [11]. All structures were solved using the Patterson method. The data were corrected for absorption by DIFABS [12]. Final full-matrix least-squares cycle included all non-hydrogen atoms with anisotropic thermal parameters and all hydrogen atoms at calculated positions using idealized geometries of 0.95 Å of C-H distance with isotropic thermal parameters which were 1.2 times the connected atoms.

2.5. Measurements

¹H NMR spectra were recorded on a JEOL α 400 spectrometer. UV-Vis absorption spectra were obtained by using a Hitachi U-3500 spectrophotometer. ESR spectra were measured on a JEOL JES-TE200 spectrometer at 77 K. Cyclic voltammetry (CV) studies were carried out by using a Hokuto HB-111 function generator and an HA-105 potentiostat/galvanostat. The working, counter and reference electrodes were a glassy carbon button, a platinum wire and a BAS RE-5 Ag⁺/Ag electrode, respectively. All the CV were measured at the potential sweep rate of 100 mV s⁻¹. For the electrolysis study the working electrode was a platinum wire and the counter was a gold wire. The supporting electrolyte was tetra-n-butylammonium hexafluorophosphate. To correct liquid junction potential, the oxidation potential of ferrocene (Fc) in the same electrolytic solution was recorded after each CV measurement and the electrode potentials were converted into those relative to Fc⁺/Fc.

3. Results and discussion

3.1. Synthesis

The reaction of $[\text{Ir}(\mu\text{-Cl})(\text{COD})]_2$ with lithium salts of aminopyridines in toluene gave $[\text{Ir}(\mu\text{-L})(\text{COD})]_2$ (**1**: L = ap, **2**: L = anp) with yields between 24 and 36%. These compounds in solution were unstable in air, but

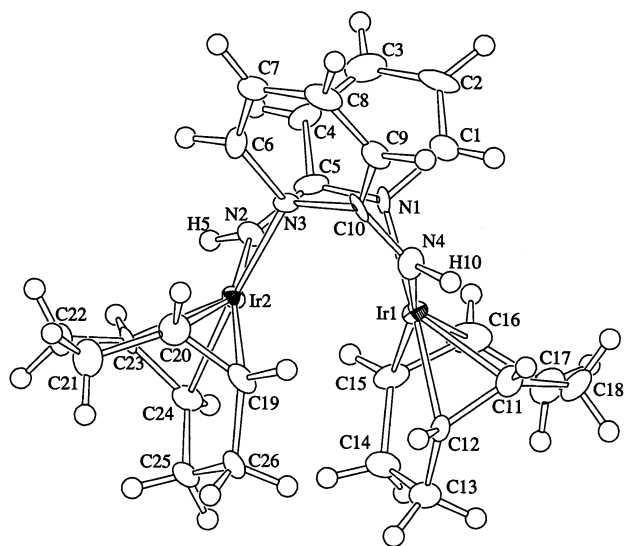


Fig. 1. ORTEP view of $[\text{Ir}(\mu\text{-ap})(\text{COD})]_2$ (**1**) with the 50% probability ellipsoids.

in crystalline form they were stable in air for at least a month.

3.2. Structure

ORTEP views of **1** and **2** are depicted in Figs. 1 and 2, respectively. Important distances and angles of **1** and **2** are summarized in Table 2. In complex **1** two iridium atoms are bridged by two aminopyridinato ligands in a head-to-tail arrangement. The coordination sphere of each Ir(I) center is square planar, which is made up of two π bonds of a chelating COD ligand, one pyridine nitrogen atom from one bridging aminopyridinato group and an amido nitrogen atom of the other. Geometry of the bridging aminopyridinato and COD ligands is normal. The average Ir–N(pyridine) distance of

Table 2

Selected bond distances (\AA) and angles ($^\circ$) for $[\text{Ir}(\mu\text{-ap})(\text{COD})]_2$ (**1**) and $[\text{Ir}(\mu\text{-anp})(\text{COD})]_2$ (**2**)

1		2	
<i>Bond distances</i>			
Ir(1)–N(1)	2.133(8)	Ir(1)–N(1)	2.125(5)
Ir(1)–N(4)	2.044(8)	Ir(1)–N(4)	2.078(5)
Ir(1)–C(11)	2.08(1)	Ir(1)–C(23)	2.109(6)
Ir(1)–C(12)	2.124(9)	Ir(1)–C(24)	2.121(6)
Ir(1)–C(15)	2.13(1)	Ir(1)–C(27)	2.125(6)
Ir(1)–C(16)	2.13(1)	Ir(1)–C(28)	2.141(6)
Ir(2)–N(2)	2.048(8)	Ir(2)–N(2)	2.098(4)
Ir(2)–N(3)	2.135(8)	Ir(2)–N(3)	2.155(5)
Ir(2)–C(19)	2.124(10)	Ir(2)–C(31)	2.120(6)
Ir(2)–C(20)	2.133(10)	Ir(2)–C(32)	2.110(6)
Ir(2)–C(23)	2.10(1)	Ir(2)–C(35)	2.111(6)
Ir(2)–C(24)	2.11(1)	Ir(2)–C(36)	2.139(6)
<i>Bond angles</i>			
N(1)–Ir(1)–N(4)	90.0(3)	N(1)–Ir(1)–N(4)	88.3(2)
N(2)–Ir(2)–N(3)	89.4(3)	N(2)–Ir(2)–N(3)	87.6(2)
Ir(1)–N(1)–C(1)	116.4(7)	Ir(1)–N(1)–C(1)	112.7(4)
Ir(1)–N(1)–C(5)	124.0(6)	Ir(1)–N(1)–C(5)	124.4(4)
Ir(1)–N(4)–C(10)	126.9(7)	Ir(1)–N(4)–C(16)	120.4(4)
Ir(2)–N(2)–C(5)	127.3(7)	Ir(1)–N(4)–C(17)	122.6(4)
Ir(2)–N(3)–C(6)	114.8(7)	Ir(2)–N(2)–C(5)	123.2(4)
Ir(2)–N(3)–C(10)	123.8(6)	Ir(2)–N(2)–C(6)	120.7(4)
N(1)–C(5)–N(2)	117.2(8)	Ir(2)–N(3)–C(12)	113.5(4)
N(3)–C(10)–N(4)	117.8(9)	Ir(2)–N(3)–C(16)	126.8(4)
		N(1)–C(5)–N(2)	117.9(5)
		N(3)–C(16)–N(4)	118.2(5)

2.134(8) \AA which is similar to those in $[\text{Ir}(\mu\text{-mhp})(\text{COD})]_2$ [4,5] and $[\text{Ir}(\mu\text{-pz})(\text{COD})]_2$ [6,7] is longer than the Ir–N(amido) distance of 2.046(8) \AA . The average Ir–C distance of 2.11(1) \AA is similar to those of reported $[\text{Ir}(\mu\text{-L})(\text{COD})]_2$ complexes [4–7]. In complex **2** the average Ir–N(pyridine) and Ir–N(amido) distances were 2.140(5) and 2.088(5) \AA , respectively. Complexes **1** and **2** have a pseudo-two-fold axis bisecting the line between the two Ir atoms. Dihedral angles between the two coordination planes of the metal atoms were 54.2 and 55.1 $^\circ$ for **1** and **2**, respectively. N1–Ir1–Ir2–N2 torsion angles for **1** and **2** were 29.3(4) and 31.3(2) $^\circ$, respectively. These dihedral and torsion angles are similar to those of $[\text{Ir}(\mu\text{-mhp})(\text{COD})]_2$ where the dihedral and torsion angles were 55.5 and 37.4(2) $^\circ$ [4]. The Ir \cdots Ir separations in **1** and **2** are 3.0998(6) and 3.0681(3) \AA , respectively (Table 3). These Ir \cdots Ir distances are very similar to each other and are shorter than 3.242(1) \AA in $[\text{Ir}(\mu\text{-mhp})(\text{COD})]_2$ [4,5] and 3.161(1) \AA in $[\text{Ir}(\mu\text{-pz})(\text{COD})]_2$ [6,7]. There is no formal Ir–Ir bond in these complexes.

3.3. Properties

The UV–Vis absorption spectra of **1** and **2** are shown in Fig. 3. The longest wavelength absorption peak was observed at 536 and 562 nm for **1** and **2**,

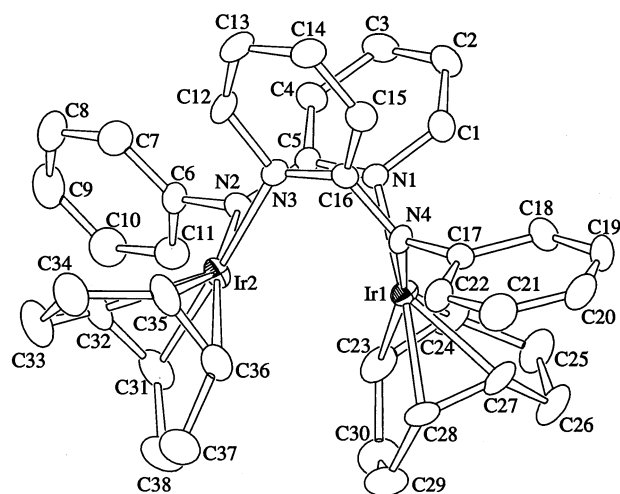


Fig. 2. ORTEP view of $[\text{Ir}(\mu\text{-anp})(\text{COD})]_2$ (**2**) with the 50% probability ellipsoids. Hydrogen atoms are omitted for clarity.

Table 3
Ir...Ir separation in $[\text{Ir}(\mu\text{-L})(\text{COD})_2]$

L	Ir...Ir (Å)	Ref.
ap	3.0998(6)	a
anp	3.0681(3)	a
pz	3.216(1)	[7]
mhp	3.242(1)	[4]
mtz	3.5434(1)	[8]
mpm	3.6806(3)	[9]

^a Present work.

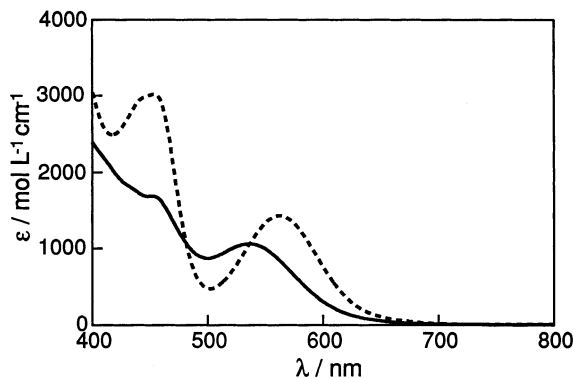


Fig. 3. UV-Vis spectra of $[\text{Ir}(\mu\text{-ap})(\text{COD})_2]$ (**1**) (solid line) and $[\text{Ir}(\mu\text{-anp})(\text{COD})_2]$ (**2**) (dotted line) in CH_2Cl_2 solution.

respectively, which is red shifted compared with those of $[\text{Ir}(\mu\text{-mhp})(\text{COD})_2]$ (484 nm) [13] and $[\text{Ir}(\mu\text{-pz})(\text{COD})_2]$ (499 nm) [14]. These bands have been assigned primarily to the metal-centered $d\sigma^* - p\sigma$ transition which has been diagnostic of the $d^8 - d^8$ interaction [13,14]. The short metal-metal separation in the present complexes causes strong $\text{M}\cdots\text{M}$ interaction and the occupied $d\sigma^*_{\text{Ir-Ir}}$ orbital would be destabilized and the unoccupied $p\sigma_{\text{Ir-Ir}}$ orbital is expected to be stabilized. As a result, the $d\sigma^* - p\sigma$ energy gap becomes smaller and the corresponding transition shifts to a longer wavelength. Thus, for the present aminopyridinato complexes the red shift of these bands is consistent with their short Ir...Ir separations.

The cyclic voltammogram of **1** in 0.1 M $n\text{-Bu}_4\text{NPF}_6/\text{CH}_2\text{Cl}_2$ exhibited a partially reversible oxidation wave at -0.41 V and an irreversible oxidation peak at 0.45 V versus Fc^+/Fc as shown in Fig. 4. Complex **2** exhibited a chemically reversible oxidation response at -0.36 V versus Fc^+/Fc followed by an irreversible oxidation peak at 0.44 V versus Fc^+/Fc (Table 4). These first oxidation potentials are about 0.3–0.5 V lower than those of $[\text{Ir}(\mu\text{-mhp})(\text{COD})_2]$ [4], $[\text{Ir}(\mu\text{-pz})(\text{COD})_2]$ [4], $[\text{Ir}(\mu\text{-form})(\text{COD})_2]$ [15] and $[\text{Ir}(\mu\text{-hp})(\text{COD})_2]$ [15]. These low oxidation potentials should be due to increased electron donor properties of the present aminopyridinato ligands in comparison to those of mhp and pz ligands and also to the upward shift of

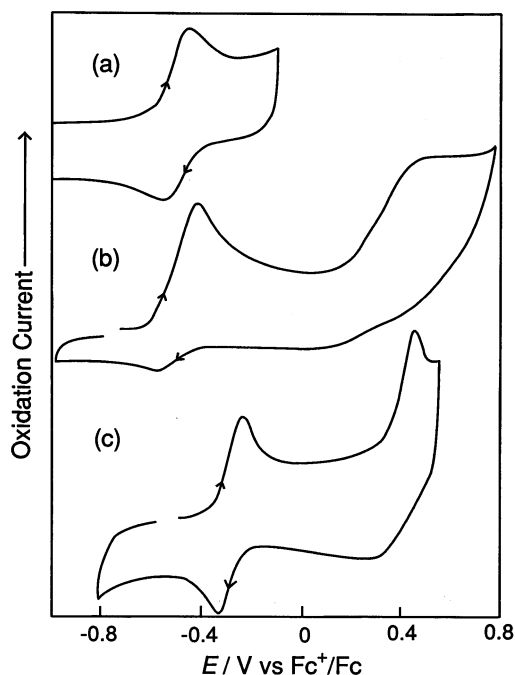


Fig. 4. Cyclic voltammogram of $[\text{Ir}(\mu\text{-ap})(\text{COD})_2]$ (**1**) (a and b) and $[\text{Ir}(\mu\text{-anp})(\text{COD})_2]$ (**2**) (c) in CH_2Cl_2 containing 0.1 M $n\text{-Bu}_4\text{NPF}_6$.

Table 4
Oxidation potentials of $[\text{Ir}(\mu\text{-L})(\text{COD})_2]$

L	$E_{1/2}^1$ (V ^a)	E_{pa}^2 (V ^{a,b})	Ref.
ap	-0.41	+0.45	c
anp	-0.36	+0.44	c
mhp	-0.13	d	[4]
pz	-0.36	d	[7]
form	0.06	d	[15]
hp	0.23	d	[15]

^a Potential vs. Fc^+/Fc .

^b Irreversible.

^c Present work.

^d Not reported.

the energy level of the $d\sigma^*$ HOMO (vide infra) induced by the short Ir...Ir separation. Electrolytic oxidation of **2** was carried out at -0.02 V versus Fc^+/Fc in $n\text{-Bu}_4\text{NPF}_6/\text{CH}_2\text{Cl}_2$. The coulometry showed that this process is a one-electron oxidation. After the electrolysis the cyclic voltammogram of the solution showed a quasi-reversible reduction wave at the same potential as the oxidation of **2**. The ESR spectrum of the electrolyzed solution frozen at 77 K was obtained as shown in Fig. 5. This spectrum is rhombic with $g_1 = 2.43$, $g_2 = 2.30$ and $g_3 = 2.08$ and hyperfine coupling was not resolved. The large shifts of the principal values of the g tensor from the free spin value ($g_e = 2.002$) shows that the odd electron of the cationic radical, $\mathbf{2}^+$, is distributed predominantly on the iridium atoms, most probably resulting in an Ir...Ir bond with a bond order

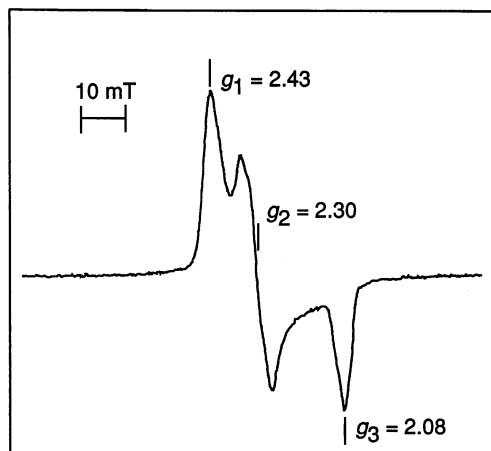


Fig. 5. X-band ESR spectrum at 77 K of $[\text{Ir}(\mu\text{-anp})(\text{COD})]_2^+$ electrolytically generated in CH_2Cl_2 containing 0.1 M $n\text{-Bu}_4\text{NPF}_6$.

of 1/2. Although the cationic radical was persistent at least for 3 days in CH_2Cl_2 in air, trials to isolate a salt of the cationic radical were unsuccessful. We are trying to prepare Ir(II) dinuclear complexes starting from the present **1** and **2** complexes encouraged by their low oxidation potentials.

4. Supplementary material

Crystallographic data (excluding structure factors) for the structures in this paper have been deposited with the Cambridge Crystallographic Data Centre as supplementary publication nos. CCDC 118695 for $[\text{Ir}(\mu\text{-ap})(\text{COD})]_2$ and CCDC 118696 for $[\text{Ir}(\mu\text{-anp})-$

$(\text{COD})]_2$. Copies of the data can be obtained free of charge on application to The Director, CCDC, 12 Union Road, Cambridge CB2 1EZ, UK (Fax: +44-1223-336-033 or e-mail: deposit@ccdc.cam.ac.uk).

Acknowledgements

We are grateful for the financial support from the Ministry of Education, Science and Culture of Japan.

References

- [1] F.A. Cotton, R.A. Walton, *Multiple Bonds Between Metal Atoms*, 2nd edn, Oxford University Press, Oxford, 1993.
- [2] F.A. Cotton, R. Poli, *Polyhedron* 6 (1987) 1625.
- [3] F.A. Cotton, R. Poli, *Inorg. Chim. Acta* 122 (1986) 243.
- [4] G.S. Rodman, K.R. Mann, *Inorg. Chem.* 24 (1985) 3507.
- [5] G.S. Rodman, K.R. Mann, *Inorg. Chem.* 27 (1988) 3338.
- [6] K.A. Beveridge, G.W. Bushnell, K.R. Dixon, D.T. Eadie, S.R. Zworotko, *J. Am. Chem. Soc.* 104 (1982) 920.
- [7] A.W. Coleman, D.T. Eadie, S.R. Stobart, *J. Am. Chem. Soc.* 104 (1982) 922.
- [8] T. Sielisch, M. Cowie, *Organometallics* 7 (1988) 707.
- [9] D.E. Chebi, P.E. Fanwick, I.P. Rothwell, *Organometallics* 9 (1990) 2948.
- [10] R.H. Crabtree, G.E. Morris, *J. Organomet. Chem.* 135 (1977) 395.
- [11] TEXSAN: Crystal Structure Analysis Package, Molecular Structure Corporation, 1985 and 1992.
- [12] N. Walker, D. Stuart, *Acta Crystallogr., Sect. A* 39 (1983) 158.
- [13] G.S. Rodman, K.R. Mann, *Inorg. Chem.* 27 (1988) 3347.
- [14] J.L. Marshall, S.R. Stobart, H.B. Gray, *J. Am. Chem. Soc.* 106 (1984) 3027.
- [15] F.A. Cotton, R. Poli, *Inorg. Chem.* 26 (1987) 590.